ON THE USE OF COLLABORATIVE SPARSE REGRESSION IN HYPERSPECTRAL UNMIXING CHAINS

Marian-Daniel Iordache[1], *Akpona Okujeni*[2], *Sebastian van der Linden*[2], *José M. Bioucas-Dias*[3], *Antonio Plaza*[4] *and Ben Somers*[5]

[1]Flemish Institute for Technological Research, Centre for Remote Sensing and Earth Observation Processes (TAP), Boeretang 200, 2400 Mol, Belgium
[2] Geography Department, Humboldt-Universität zu Berlin, Unter den Linden 6, 10099 Berlin, Germany
[3] Instituto de Telecomunicações and Instituto Superior Técnico, ULisboa, 1049-001, Lisbon, Portugal
[4] Hyperspectral Computing Laboratory, Department of Technology of Computers and Communications, University of Extremadura, E-10071 Cáceres, Spain
[5] Department Earth and Environmental Sciences, Division Forest, Nature and Landscape, KU Leuven, Celestijnenlaan 200E - bus 2411, B-3001 Leuven, Belgium

ABSTRACT

Hyperspectral unmixing is a complex process in which several steps are consecutively executed to derive the desired results: the image endmembers and their corresponding fractional abundance maps. Each of these unmixing stages benefits nowadays from a plethora of algorithms, continuously developed and improved. In this paper, we analyze three of the general unmixing steps: band selection (data dimensionality reduction), endmember extraction and fractional abundance inference (inversion) from a multi-measurement vector problem point of view. We show that these particular steps can be expressed as a convex optimization problem in which the concept of data collaborativity is exploited and one single algorithm can be efficiently used to solve them. Our experimental results obtained in an urban dataset acquired over Berlin, Germany, show the potential of this approach in remote sensing applications.

Index Terms— Unmixing, sparse regression, MMV, data collaborativity

1. INTRODUCTION

In hyperspectral unmixing, several processing steps are performed in order to derive the pure materials in the scene (*endmember extraction*) and the area they occupy inside each pixel of the image (*fractional abundances inference*) [1–3]. For computational purposes, a data dimensionality reduction method is sometimes applied as a pre-processing step to the data expressed in reflectance units (see, *e.g.*, [4]). Many methods and algorithms are available in the literature for each of the aforementioned tasks. The data dimensionality reduction mainly relies on the fact that the number of available bands is much larger than the dimensionality of the space spanned by the data, which is one less than equal to the number of endmembers. Endmember extraction can be tackled through geometrical, statistical or sparse regression methods. The inversion step estimates the fractional abundances of the endmembers and it is performed normally by solving convex optimization problems in which constrained solutions are derived. For a comprehensible overview of the aforementioned methods, the reader might refer to [5].

In this work, we tackle three specific unmixing tasks (band selection - which is a dimensionality reduction step, endmember extraction and inversion) from a *multi–measurement vector* (MMV) point of view. Our approach is inspired by the sparse regression unmixing approach, in which only a few atoms out of a large spectral library contribute to the observed data.

2. COLLABORATIVE SPARSE REGRESSION

In this paper, we assume that the observed spectra are modeled by the linear mixing model, such that each vector can be expressed as a linear combination of the spectra of constituent endmembers, weighted by their corresponding fractional abundances. In the recent years, the unmixing problem was tackled in a semi-supervised fashion, by assuming that the endmembers spectra are present in a large collection of pure spectra (*spectral library* or *dictionary*) [6].

Let L be the number of spectral bands and $\mathbf{A} := [\mathbf{a}_1, \ldots, \mathbf{a}_m] \in \mathbb{R}^{L \times m}$ a spectral library with m spectral signatures available *a priori*. Assuming that the data set contains $n \gg L$ pixels organized in the matrix $\mathbf{Y} := [\mathbf{y}_1, \ldots, \mathbf{y}_n]$, we can write

$$\mathbf{Y} = \mathbf{A}\mathbf{X} + \mathbf{N}, \tag{1}$$

where $\mathbf{X} := [\mathbf{x}_1, \ldots, \mathbf{x}_n]$ is the abundance fraction matrix and $\mathbf{N} := [\mathbf{n}_1, \ldots, \mathbf{n}_n]$ is the noise matrix. The fractional abundances should be non-negative (ANC) and sum to one (ASC) in each pixel, due to physical constraints. Herein, we do not use the ASC as, due to various factors, such as topographic modulation and spectral variability, it is often violated. See [5] for details. We can formulate the unmixing as a multi-measurement vector (MMV) problem (see [7–9] and references therein), which, formally, corresponds to finding the solution of the optimization

$$\min_{\mathbf{X}} \|\mathbf{X}\|_0 \;\text{ subject to: }\; \mathbf{Y} = \mathbf{A}\mathbf{X}, \tag{2}$$

This work has been supported by the European Community's Marie Curie Research Training Networks Programme under contract MRTN-CT-2006-035927, Hyperspectral Imaging Network (HYPER-I-NET). Funding from Fundação para a Ciência e Tecnologia, Portuguese Ministry of Science and Higher Education (projects PEst-OE/EEI/0008/2013 and SFRH/BD/87693/2012) and from the Spanish Ministry of Science and Innovation (CEOS-SPAIN project, reference AYA2011-29334-C02-02) is also gratefully acknowledged.

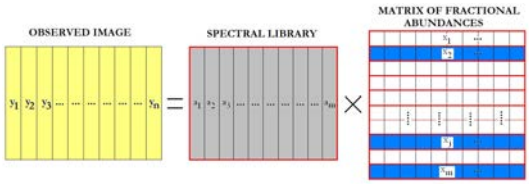

Fig. 1. Data collaborativity when a spectral library is available.

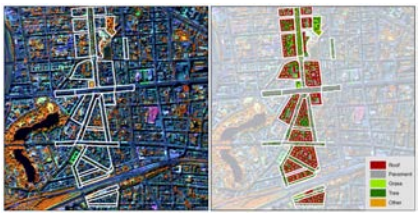

Fig. 2. HyMap subset and reference polygons for validation.

where $\|\mathbf{X}\|_0 := |S|$, $S := \text{supp}(\mathbf{X}) := \{1 \leq i \leq m : \mathbf{x}^i \neq \mathbf{0}\}$, and $\mathbf{x}^i$ is the ith row of $\mathbf{X}$.

In other words, the solution of the optimization problem (2) is the matrix of fractional abundances $\mathbf{X}$ which perfectly explains the observed data by using the minimum number of active library spectra (*i.e.*, library atoms which have at least one non-zero value in the corresponding row from $\mathbf{X}$). An illustration is given in Fig. 1.

However, the optimization problem (2) is non-convex and a perfect reconstruction of the observed data is not possible due to the existence of noise (as shown in (1)). It was shown [10] that the solution of (2) can be recovered with high accuracy by solving the following equivalent convex optimization problem:

$$\begin{aligned} \min_{\mathbf{X}} \quad & \|\mathbf{Y} - \mathbf{A}\mathbf{X}\|_F^2 + \lambda \|\mathbf{X}\|_{2,1} \\ \text{subject to:} \quad & \mathbf{X} \geq 0, \end{aligned} \tag{3}$$

where $\|\mathbf{X}\|_{2,1} := \sum_{i=1}^{m} \|\mathbf{x}^i\|_2$ is the mixed $\ell_{2,1}$ norm, which promotes sparsity among the rows of $\mathbf{X}$, λ is a regularization parameter setting the relative weight between the data term and the $\ell_{2,1}$ mixed norm, and the ANC is enforced. Problem (3) is similar to the collaborative sparse coding problem described in [9, 11–13]. The main difference is the introduction of the constraint $\mathbf{X} \geq 0$ (see [10] for more details). In this paper, we use the *Collaborative Sparse Unmixing via variable Splitting and Augmented Lagrangian* (CLSUnSAL) algorithm [10] to solve optimization problem (3).

Next, we show how the convex optimization problem (3) can be employed in three major unmixing steps: endmember extraction, band selection (data dimensionality reduction) and inversion.

2.1. Collaborative endmember extraction

Fig. 1 suggests that, from the available spectral library, only a few atoms contribute to the observed data. We deduce that these atoms can only be the endmembers. However, we can easily imagine a situation in which we do not have a spectral library at our disposal. In this case, we use the image $\mathbf{Y}$ as a *self–dictionary*. It was shown in [14] that, in this case, the problem (2) in data uncontaminated with noise can be solved through greedy approaches, equivalent to other well-known methods. Here, we will use CLSUnSAL to solve the optimization problem (3) when the library $\mathbf{A}$ is replaced with the self–dictionary $\mathbf{Y}$ (the image itself).

2.2. Collaborative band selection

The sparse collaborative model can be used to select representative bands from a datacube by transposing the input image in the convex optimization problem (3), which can be thus rewritten as: $\min_{\mathbf{X}} \|\mathbf{Y}' - \mathbf{Y}'\mathbf{X}\|_F^2 + \lambda\|\mathbf{X}\|_{2,1}$ subject to: $\mathbf{X} \geq 0$. Each column of the transposed matrix ($\mathbf{Y}'$) contains the reflectance values of all the image pixels at the corrresponding spectral band. CLSUnSAL was used in [15] to refine selected bands obtained by an N-FINDR with band linear prediction (N-FINDR+LP) [16] approach. In this paper, we apply CLSUnSAL to directly reduce the number of bands from the observed data.

2.3. Collaborative sparse regression (inversion)

CLSUnSAL was originally designed to perform hyperspectral unmixing when a spectral library is available. Here, the algorithm input in the inversion stage consists of the reference library and the matrix of selected endmembers, in turn.

3. EXPERIMENTAL RESULTS IN REAL DATA

The dataset used in our experiments is a 516×514 subset of a hyperspectral image covering the city of Berlin, Germany (see Fig. 2 – left). The scene was acquired by the HyMap sensor in 125 spectral bands, with a spatial resolution of 3.6m. A total number of 41 spectra from a comprehensive spectral library were selected as pure signatures of endmembers on the ground. The spectral library was developed from the image on the basis of expert knowledge and auxiliary information (field mapping data, Google Street View). The library spectra are categorized into four spectrally complex and similar urban land cover classes, *i.e.* roof and pavement as well as grass and tree. An extensive overview of the characteristics of the image, image-preprocessing and library development can be found in [17].

The ground-truth abundance fractions corresponding to the urban land cover classes are known in the considered image at a block level, as shown in Fig. 2 (left – positioning of the polygons in the image; right – dominant classes inside the polygons; for more details, see [17]).

Next, we report the performances achieved by CLSUnSAL for the different unmixing stages. For clarity, the regularization parameter λ will be respectively reported as: λ_b for band selection, λ_e for endmember extraction and λ_i for inversion.

3.1. Band selection

The methodology described in Section 2.2 is applied to the input image using several values of the regularization parameter λ_b in CLSUnSAL objective function: 5, 10, 15, 20, 25. Using the retained spectral bands and the corresponding coefficients, we then reconstruct the original datacube and we measure the quality of the reconstruction by means of the *signal-to-reconstruction error*: $\text{SRE} \equiv E[\|\mathbf{y}\|_2^2]/E[\|\mathbf{y} - \widehat{\mathbf{y}}\|_2^2]$, measured in dB: $\text{SRE(dB)} \equiv 10\log_{10}(\text{SRE})$.

Table 1 shows the number of retained spectral bands and the SRE(dB) for the considered values of λ_b. As expected, the quality of the reconstruction decreases when less spectral bands are retained (with increasing λ_b). However, even for a significant reduction of the number of bands, the reconstruction of the dataset has a good quality performance, as exemplified in Fig. 3. In this figure, the plot at the

Table 1. Number of retained bands and SRE(dB) for different values of the parameter λ_b.

λ	5	10	15	20	25
# bands	114	87	63	60	57
SRE(dB)	36.43	31.61	29.89	29.86	28.77

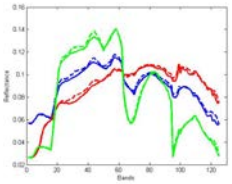

(a) Original (continuous) and reconstructed (dashed) spectra

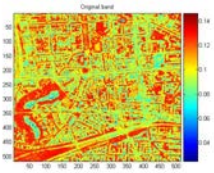

(b) Original band

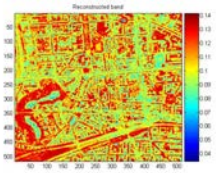

(c) Reconstructed band

Fig. 3. Comparison between original and reconstructed data after band selection ($\lambda_b = 20$).

top (Fig. 3.(a)) shows the signatures of three random pixels from the original image (continuous line) and their reconstructed correspondents, while the bottom part (Figs. 3.(b)–(c)) displays a randomly chosen (and not selected) band of the dataset when only 60 bands are retained (*i.e.*, for $\lambda_b = 20$) and its reconstructed correspondent. Note the high similarity between the reconstructed data and the original one, which was expected, given that previous work [6] reports that a level of 5dB for SRE(dB) (computed there on real and estimated fractional abundances) leads to a useful reconstruction of the observed spectrum. Note that the values in Table 1 are much above this limit.

3.2. Endmember extraction

In our previous work [14], we have reported endmember extraction results in the considered dataset for two values of the regularization parameter λ_e: 1 and 5. CLSUnSAL was applied at sub-image level (the image being split in 100 sub-images of 2500 pixels approximatively each), due to memory usage constraints, and all the extracted spectra were put together to build the inferred mixing matrix. As a result, a large number of spectra was selected, due to the fact that most of the endmembers are repeated in several subsets. We follow here the same strategy by applying the endmember extraction methodology on the reduced dataset with 63 bands, obtained after band selection when $\lambda_b = 15$. As in [14], we do not investigate methods to refine this matrix, but we rely on the available ground-truth spectra to select the most correlated three extracted endmembers to each library member in terms of spectral angle distance (SAD). Thus, a new library containing 123 spectra is created.

In Fig. 4, we display the following: left – ground-truth (red) and most similar extracted spectra (blue) without band selection; right – the corresponding plots after using band selection and reconstructing the spectra, for the four considered classes of endmembers. In all

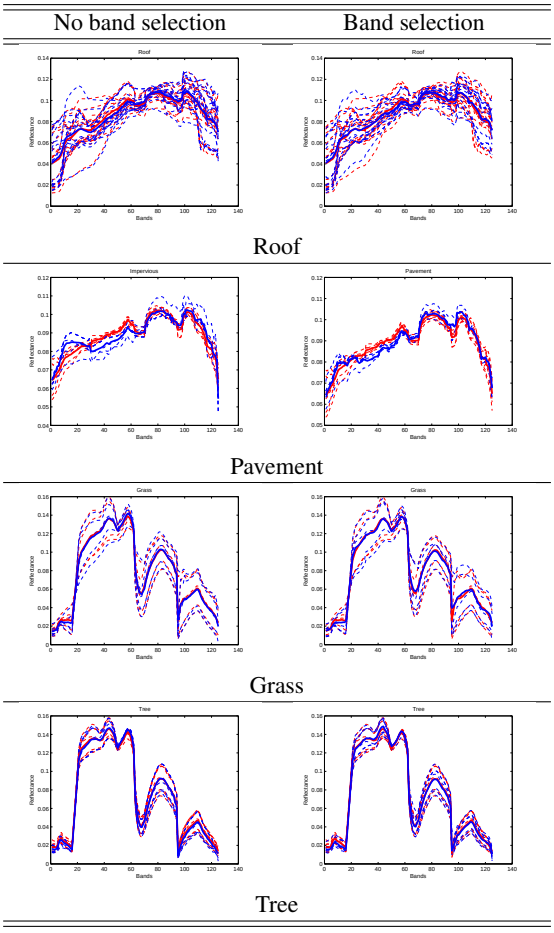

Fig. 4. Quality of the extracted endmembers without (left) and with (right) band selection when $\lambda_e = 1$.

plots, the thick line corresponds to the mean spectrum (red – ground-truth, blue – extracted). The regularization parameter for endmember extraction is set to $\lambda_e = 1$ for all subsets, in both cases. Note the high correlation between the reference and extracted spectra in both cases. Also, there are no significant differences between the extracted spectra when the full and the reduced datasets are employed. A slight change is visible only for the pavement signatures. However, previous work [17] shows that this class is unmixed with less accuracy than other classes in the given dataset, due to spectral similarities to other classes, ambiguities and shadowing. In the following subsection, devoted to the inversion step, we report unmixing acuracies obtained when the reference and the extracted spectra are used in turn as input to CLSUnSAL.

3.3. Inversion

We compare here the unmixing accuracies of CLSUnSAL when the reference and the extracted libraries are employed. The extracted library consists of a set of 123 spectra in which each signature from the reference library corresponds to the three most similar extracted signatures in terms of spectral angle distance (SAD). The regularization parameter λ_i was empirically set to 0.01 for the original library and 0.05 for the extracted library. Fig 5 shows the accuracy of fraction maps evaluated by comparing modeled versus reference

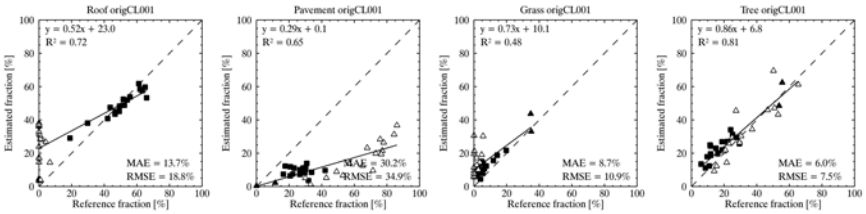

(a) Original library (from left to right: roof, pavement, grass, tree)

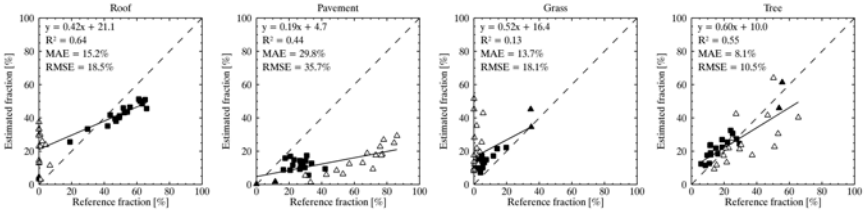

(b) Extracted library (from left to right: roof, pavement, grass, tree)

Fig. 5. CLSUnSAL performance when using as input: a) original library ($\lambda_i = 0.01$) and b) extracted library ($\lambda_i = 0.05$).

fractions using polygonwise averages. Reference data is shown in Fig. 2. Reference fractions per polygon were available for 35 polygons, including building blocks (black squares), streets (with triangles) and green spaces (black triangles). In Fig. 5, note that, despite a slight degradation of the unmixing quality when the extracted library is used instead of the reference library, the results follow the same trend, in line with the ones reported in [17].

4. CONCLUSIONS AND FUTURE WORK

In this paper, we have formulated the three typical steps of spectral unmixing (data dimensionality reduction, endmember extraction, inversion) under an MMV approach. One unique algorithm, CLSUnSAL, was applied using different configurations of the input matrices to solve, based on data collaborativity, the resulting convex optimization problems. The results obtained in a real dataset show that the proposed approach can be successfully applied in remote sensing applications. A more indepth analysis of the complete hyperspectral unmixing chain based on one single algorithm is part our future research directions. The implementation of the employed algorithm in other programming environments is also desirable, such that complete images (or larger image parts) could be used as input.

5. REFERENCES

[1] N. Keshava and J. Mustard, "Spectral unmixing," *IEEE Signal Processing Magazine*, vol. 19, no. 1, pp. 44–57, 2002.

[2] D. Landgrebe, *Signal theory methods in multispectral remote sensing*, John Wiley & Sons: New York, 2003.

[3] C.-I. Chang, *Hyperspectral imaging: techniques for spectral detection and classification*, Kluwer Academic/Plenum Publishers: New York, 2003.

[4] J. Harsanyi and C.-I. Chang, "Hyperspectral image classification and dimensionality reduction: an orthogonal subspace projection," *IEEE Trans. Geosci. Remote Sens.*, vol. 32, pp. 779–785, 1994.

[5] J. M. Bioucas-Dias, A. Plaza, N. Dobigeon, M. Parente, Q. Du, P. Gader, and J. Chanussot, "Hyperspectral unmixing overview: Geometrical, statistical and sparse regression-based approaches," *IEEE Journal of Selected Topics in Applied Earth Observations and Remote Sensing*, vol. 5, no. 2, pp. 354–379, 2011.

[6] M.-D. Iordache, J. Bioucas-Dias, and A. Plaza, "Sparse unmixing of hyperspectral data," *IEEE Transactions on Geoscience and Remote Sensing*, vol. 49, no. 6, pp. 2014–2039, 2011.

[7] J. M. Kim, O. K. Lee, and J. C. Ye, "Compressive music with optimized partial support for joint sparse recovery," *arXiv:1102.3288v2*, June 2011.

[8] M.-D. Iordache, J. Bioucas-Dias, A. Plaza, and B. Somers, "Music-csr: Hyperspectral unmixing via multiple signal classification and collaborative sparse regression," *IEEE Transactions on Geoscience and Remote Sensing (accepted)*, 2014.

[9] Y. Eldar and H. Rauhut, "Average case analysis of multichannel sparse recovery using convex relaxation," *IEEE Transactions on Information Theory*, vol. 56, no. 1, pp. 505–519, 2010.

[10] M.-D. Iordache, J.M. Bioucas-Dias, and A. Plaza, "Collaborative sparse regression for hyperspectral unmixing," *IEEE Transactions on Geoscience and Remote Sensing*, vol. 52, pp. 341–354, 2014.

[11] J. Tropp, "Algorithms for simultaneous sparse approximation. part ii: Convex relaxation," *Signal Processing*, vol. 86, no. 3, pp. 589–602, 2006.

[12] M. Mishali and Y. Eldar, "Reduce and boost: Recovering arbitrary sets of jointly sparse vectors," *IEEE Transactions on Signal Processing*, vol. 56, no. 10, pp. 4692–4702, October 2008.

[13] B. Turlach, W. Venables, and S. Wright, "Simultaneous variable selection," *Technometrics*, vol. 27, pp. 349–363, 2004.

[14] F. Xiao, W.-K. Ma, T.-H. Chan, J.M. Bioucas-Dias, and D. Iordache, "Greedy algorithms for pure pixels identification in hyperspectral unmixing: A multiple-measurement vector viewpoint," *21st European Signal Processing Conference (EUSIPCO)*, Marrakech, Morocco, 2013.

[15] Q. Du, J.M. Bioucas-Dias, and A. Plaza, "Hyperspectral band selection using a collaborative sparse model," *IEEE International Geoscience and Remote Sensing Symposium (IGARSS)*, pp. 3054–3057, July 2012.

[16] Q. Du and H. Yang, "Similarity-based unsupervised band selection for hyperspectral image analysis," *Geoscience and Remote Sensing Letters, IEEE*, vol. 5, no. 4, pp. 564–568, Oct 2008.

[17] A. Okujeni, S. van der Linden, L. Tits, B. Somers, and P. Hostert, "Support vector regression and synthetically mixed training data for quantifying urban land cover," *Remote Sensing of Environment*, vol. 137, pp. 184 – 197, 2013.